Supplement of Weather Clim. Dynam., 5, 1137–1151, 2024
https://doi.org/10.5194/wcd-5-1137-2024-supplement

Supplement of

Spatial and temporal variability of the freezing level in Patagonia's atmosphere

Nicolás García-Lee et al.

Correspondence to: Nicolás García-Lee (ngarcia@cecs.cl)

Supplementary Material

- **Tables**

Table S1. Average ($\overline{H}_0$, m a.s.l.) and Trend values ($\overline{T}$, $m\ decade^{-1}$) obtained annually and seasonally only from H_0 observation data at 12Z. Only trends with p-value < 0.05, are showed. Note that the periods are the same as those indicated in Table 1 for each location. However, the number of observations (n_{obs}) is higher because data are not filtered to match the H_0^{ERA5} database, where values of -1 are assigned as missing data.

	n_{obs}	$\overline{H}_0^{Annual}$	$\overline{H}_0^{DJF}$	$\overline{H}_0^{MAM}$	$\overline{H}_0^{JJA}$	$\overline{H}_0^{SON}$	$\overline{T}_{Annual}$	$\overline{T}_{DJF}$	$\overline{T}_{MAM}$	$\overline{T}_{JJA}$	$\overline{T}_{SON}$
Puerto Montt	27524	2311.4	3032.7	2589.9	1695.1	1990.8	25.5	60	49.4	-	-
Comodoro Rivadavia	20806	2093.2	2675.2	2275.4	1559.4	1919.4	19.1	49.5	42.9	22.7	29.6
Río Gallegos	3664	1465.1	1772.9	1402.9	1047.8	1396.4	-	-	-	-	-
Punta Arenas	12095	1283.9	1557.4	1404.9	930.2	1093.4	-	-	-	-	-

Table S2. Statistics of the seasonal validation performed between H_0 data (m a.s.l.) obtained from radiosonde data and ERA5 reanalysis data.

	MBE^{DJF}	MBE^{JJA}	r^{DJF}	r^{JJA}	$RMSE^{DJF}$	$RMSE^{JJA}$	σ_{IGRA}^{DJF}	σ_{ERA5}^{DJF}	σ_{IGRA}^{JJA}	σ_{ERA5}^{JFA}
Puerto Montt	-21.3	-41.8	0.95	0.95	282.3	224	859.7	891.3	707.9	712
Comodoro Rivadavia	-40.5	-29.1	0.95	0.95	248	244.1	765.6	776.4	738.4	757.6
Río Gallegos	-190.1	-13.3	0.86	0.69	406.6	481.4	687.1	641.5	626.2	596.4
Punta Arenas	-109.7	-123	0.95	0.87	237.9	287.9	769.2	680.1	521.5	509.1

Table S3. Statistics of the values of the 0°C isotherm (m a.s.l.) obtained in annual and seasonal format. The values shown correspond to the temporal and spatial mean ($\overline{H}_0$), median ($\widetilde{H}_0$), maximum ($H_0^{Max.}$) and minimum ($H_0^{Min.}$) of daily freezing levels values. Additionally, 75th percentile (P_{75}) and 25th percentile (P_{25}) are showed.

	$\overline{H}_0$	$\widetilde{H}_0$	$H_0^{Max.}$	$H_0^{Min.}$	P_{75}	P_{25}
Summer	2236	2130.1	3346.2	1227.6	3034.1	1402.1
Autunm	1891	1722.3	2870	1068.3	2577.6	1124
Winter	1169	968.9	1981.8	575.4	1508.7	588
Spring	1477	1312.1	2440	728.3	1949.9	874.4
Annual	1691	1519.2	2657.7	913.1	2126.5	1196

Table S4. Statistics of 0°C isotherm values (m a.s.l.) are presented in both annual and seasonal format. he interquartile range of the freezing level data (IQR) is depicted. Additionally, the average interquartile range for both latitudinal (IQR_m) and longitudinal profiles (IQR_z) is provided. Through the representation of the average ($\bar{H}_0$), maximum, and minimum values, the variability is captured for each profile.

	IQR	$\overline{IQR}_m$	$\overline{IQR}_z$	Max. ($\bar{H}_{0,m} + IQR_m$)	Min. ($\bar{H}_{0,m} - IQR_m$)	Max. ($\bar{H}_{0,z} + IQR_z$)	Min. ($\bar{H}_{0,z} - IQR_z$)
Summer	1632	290.8	929.7	3383.3	1187.5	3383.3	931.3
Autunm	1453.6	216.5	753.8	2848.2	1065.7	2858.1	841.4
Winter	920.7	159	500.3	1798.8	590.7	1930.7	446.7
Spring	1075.5	374.1	595.3	2448.5	701.1	2440.9	596.1
Annual	930.4	257.2	694.9	2625.9	904.8	2654.2	705.4

Table S5. Trends values ($m\ decade^{-1}$) obtained from each season. IQR range corresponds to the range obtained from trend values for latitudinal (IQR_m) and longitudinal profile (IQR_z). Trough the maximum and minimum the variability is represented. Only trends with p-value < 0.05, are showed.

	$\bar{T}_0$	$T_0^{Max.}$	$T_0^{Min.}$	Max. ($\bar{T}_{0,m} + IQR_m$)	Min. ($\bar{T}_{0,m} - IQR_m$)	Max. ($\bar{T}_{0,z} + IQR_z$)	Min. ($\bar{T}_{0,z} - IQR_z$)
Summer	39.8	60.7	18.1	58.3	18.6	68.2	18.6
Autunm	35.5	45.5	17.5	44.8	17.3	46.4	22.6
Winter	19	30.1	8.4	31.1	10.2	29.5	8.9
Spring	16.2	22.4	10.5	21	10.6	23.4	11.9
Annual	23.8	36.5	8.8	41	6	35.3	9.9

- **Figures**

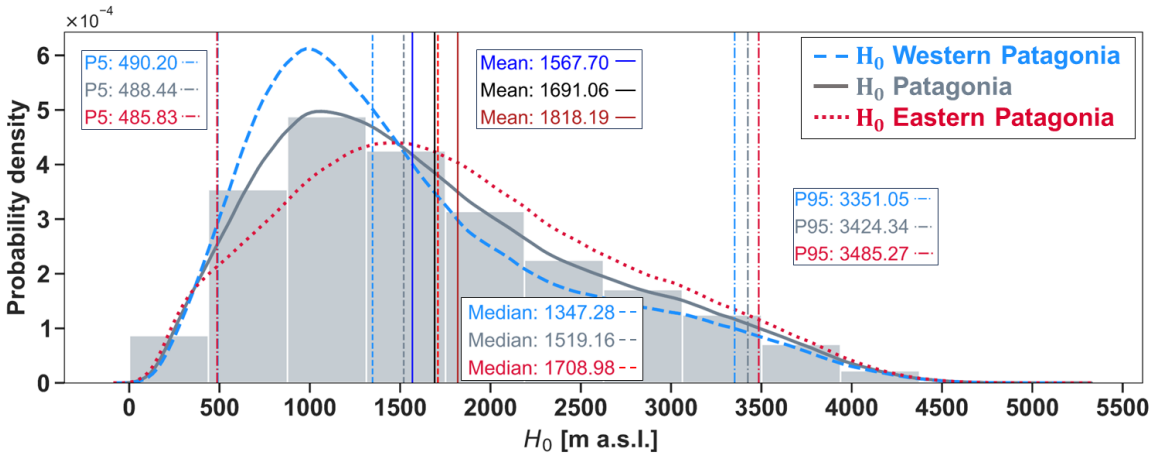

Figure S1. Histogram of ERA5 daily H_0 data in Patagonia. The gray bars represent the daily values of H_0 obtained from the spatial average across the entire study area from 1959 to 2021. The curves, indicate the fit of the kernel density estimation for the entire region (gray), Western Patagonia (blue), and Eastern Patagonia (red). Vertical lines represent the 95th percentile (P95, right dashdot line), 5th percentile (P5, left dashdot line), mean (solid), and the median (dashed) of H_0 values, each calculated within their respective regions.

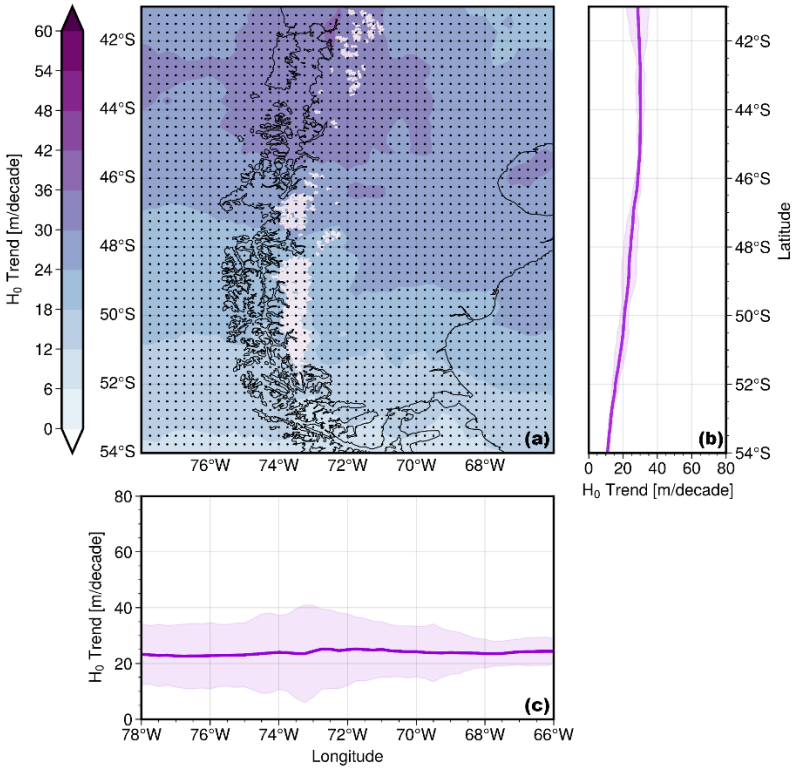

Figure S2: Spatial distribution of the 0°C isotherm trends (T_0) across the year. Lighter areas depict a lower altitude of the trends, while purple areas indicate higher values. The white contours delineate the extent of ice coverage in the region. Each distribution is accompanied by a latitudinal profile (b) and a longitudinal profile (c), showcasing the spatially averaged H_0 trend values. The purple shaded area in these profiles represents the respective interquartile range for each profile ($IQR_{m,z}$). Black circles denote statistically significant trends at p-value < 0.05.

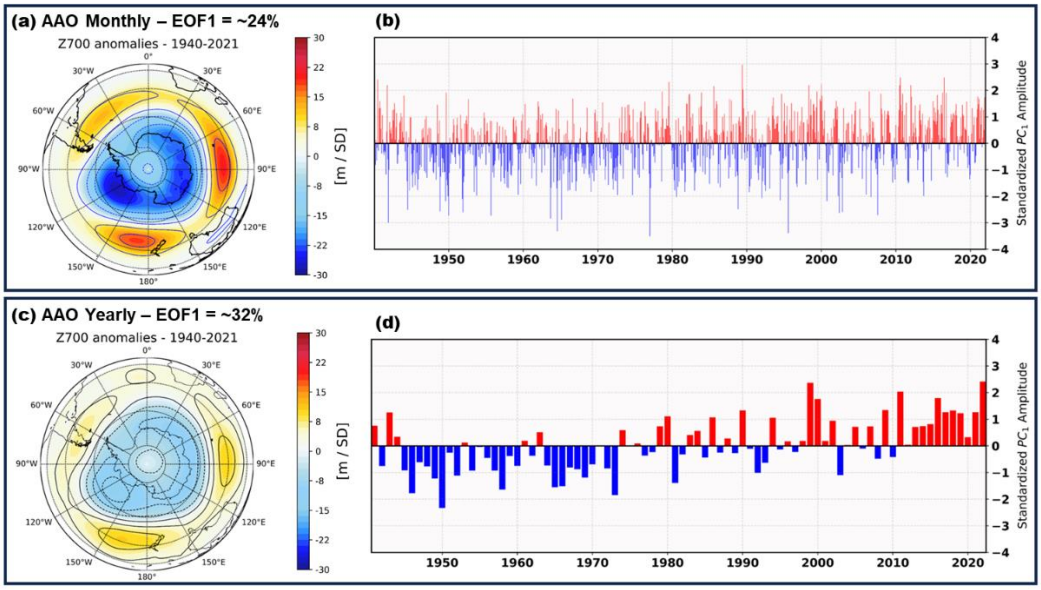

Figure S3. Leading Empirical Orthogonal Function (EOF_1) of ERA5 700 hPa geopotential height through two datasets: (a) monthly mean data, and (c) annual mean data spanning from 1940 to 2021. The EOFs are generated from detrended 700 hPa geopotential height anomaly data, weighted by the square root of the cosine of latitude, within the latitude range of 20° to 90°S. The resulting patterns are displayed as regression maps, depicting the interplay between the leading Principal Component (PC_1) time series and the spatial distribution of the evolving height anomalies (b and d, respectively). The temporal pattern is illustrated by blue and red bars (negatives/positive values) of the first Principal Component, scaled to unit variance (divided by the square root of its eigenvalue). Each panel includes insights into the proportion of explained variance and showcases the standardized PC time series grounded in the NOAA Climate Prediction Center's (CPC) 1979-2000 reference period.

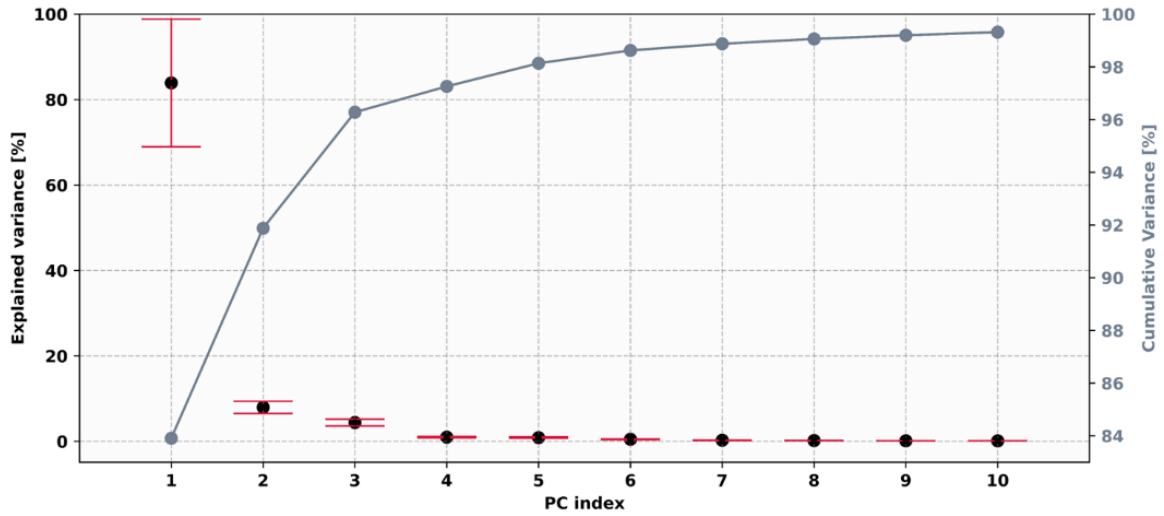

Figure S4. Eigenvalues of the top ten leading modes of variability for the annual H_0 field in Patagonia, obtained through the EOF analysis (black dots), and their associated typical errors (red bars), following the method of North et al., (1982). Moreover, the accumulated percentage of the total variance explained by each principal component (gray dots) is depicted on the right axis.

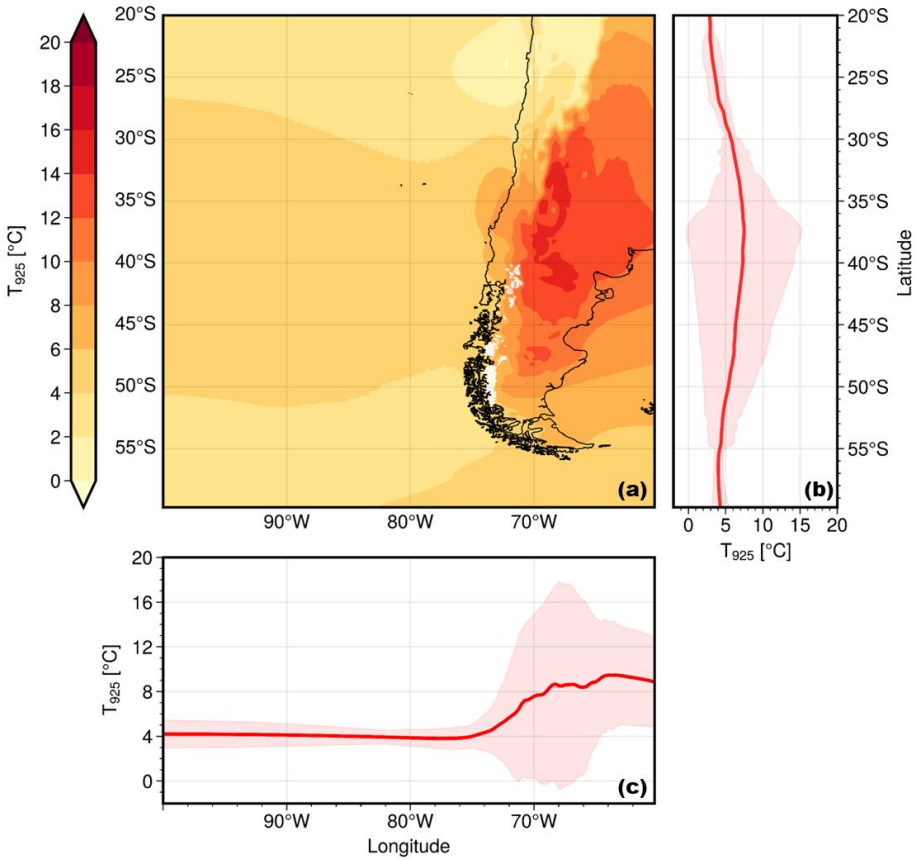

Figure S5. Spatial distribution of the January minus July mean air temperature at 925 hPa. Lighter areas depict a lower temperature, while red areas indicate higher values. The white contours delineate the extent of ice coverage in the region. Each distribution is accompanied by a latitudinal profile (b) and a longitudinal profile (c), showcasing the spatially averaged temperature values. The red shaded area in these profiles represents the respective interquartile range for each profile ($IQR_{m,z}$).

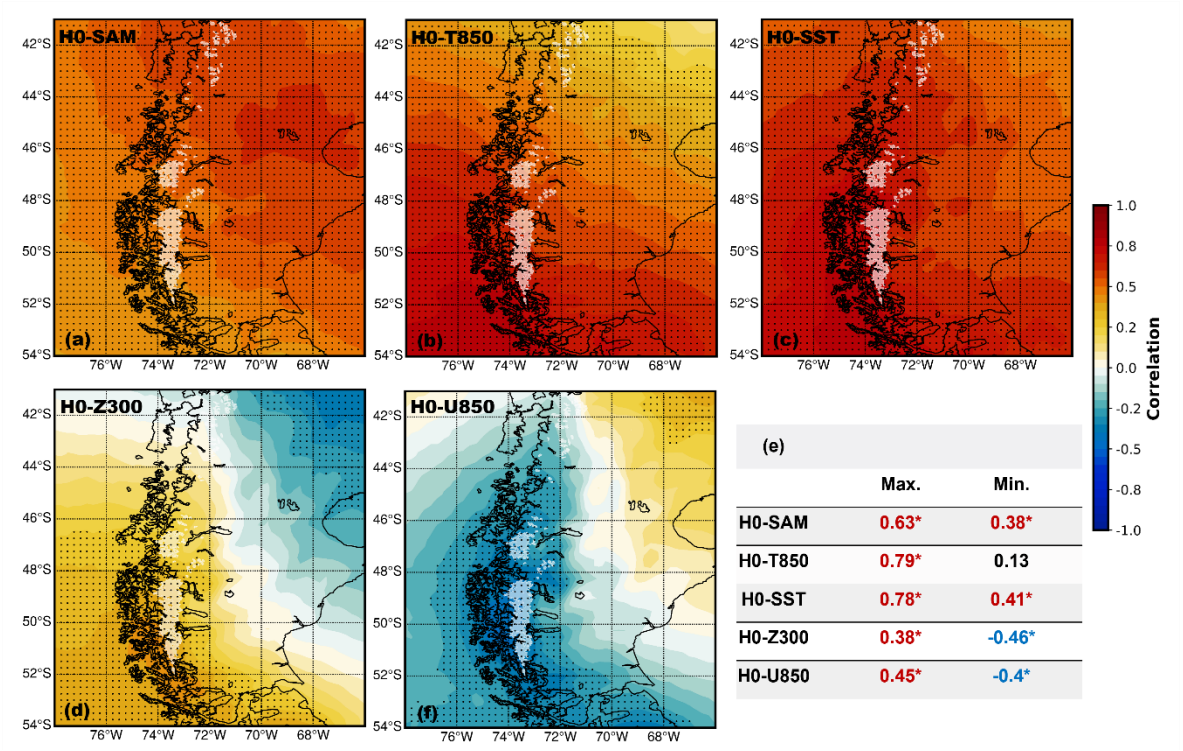

(e)

	Max.	Min.
H0-SAM	0.63*	0.38*
H0-T850	0.79*	0.13
H0-SST	0.78*	0.41*
H0-Z300	0.38*	-0.46*
H0-U850	0.45*	-0.4*

Figure S6. Spatial correlation maps between the detrended annual mean isotherm field and the detrended custom indices timeseries SAM (a), T850 (b), SST (c), Z300 (d), and U850 (f). The white contours outline the ice coverage boundaries within the region. Black circles denote statistically significant correlations. (e) Correlation chart with the maximum and minimum values of every spatial field showed, where the asterisk symbol (*) indicates statistical significance (p-value < 0.05). Red (blue) correlation values depicted positive (negative) correlations.